

# The nature of LINER galaxies:

## Ubiquitous hot old stars and rare accreting black holes

R. Singh<sup>1</sup>\*, G. van de Ven<sup>1</sup>, K. Jahnke<sup>1</sup>, M. Lyubenova<sup>1</sup>, J. Falcón-Barroso<sup>2,3</sup>, J. Alves<sup>4</sup>, R. Cid Fernandes<sup>5</sup>, L. Galbany<sup>6</sup>, R. García-Benito<sup>7</sup>, B. Husemann<sup>8</sup>, R. C. Kennicutt<sup>12</sup>, R. A. Marino<sup>13</sup>, I. Márquez<sup>7</sup>, J. Masegosa<sup>7</sup>, D. Mast<sup>7,9</sup>, A. Pasquali<sup>10</sup>, S. F. Sánchez<sup>7,9</sup>, J. Walcher<sup>8</sup>, V. Wild<sup>11</sup>, L. Wisotzki<sup>8</sup>, B. Ziegler<sup>4</sup>, and the CALIFA collaboration

(Affiliations can be found after the references)

Received 12/06/2013; accepted 08/08/2013

### ABSTRACT

*Context.* Galaxies, which often contain ionised gas, sometimes also exhibit a so-called low-ionisation nuclear emission line region (LINER). For 30 years, this was attributed to a central mass-accreting supermassive black hole (more commonly known as active galactic nucleus or AGN) of low luminosity, making LINER galaxies the largest AGN-sub-population, which dominate in numbers over higher luminosity Seyfert galaxies and quasars. This, however, poses a serious problem. While the inferred energy balance is plausible, many LINERs clearly do not contain any other independent signatures of an AGN.

*Aims.* Using integral field spectroscopic data from the CALIFA survey, we compare the observed radial surface brightness profiles with what is expected from illumination by an AGN.

*Methods.* Essential for this analysis is a proper extraction of emission lines, especially weak lines, such as Balmer H $\beta$  lines which are superposed on an absorption trough. To accomplish this, we use the GANDALF code, which simultaneously fits the underlying stellar continuum and emission lines.

*Results.* For 48 galaxies with LINER-like emission we show, that the radial emission-line surface brightness profiles are inconsistent with ionisation by a central point-source and hence cannot be due to an AGN alone.

*Conclusions.* The most probable explanation for the excess LINER-like emission is ionisation by evolved stars during the short but very hot and energetic phase known as post-AGB. This leads us to an entirely new interpretation. Post-AGB stars are ubiquitous and their ionising effect should be potentially observable in every galaxy with the gas present and with stars older than  $\sim 1$  Gyr unless a stronger radiation field from young hot stars or an AGN outshines them. This means that galaxies with LINER-like emission are not a class defined by a property but rather by the absence of a property. It also explains why LINER emission is observed mostly in massive galaxies with old stars and little star formation.

**Key words.** galaxies: active – galaxies: nuclei – galaxies: ISM – stars: AGB and post-AGB

## 1. Introduction

When LINERs were first identified as a class of galaxies in the early 1980s, it was clear that the necessary radiation field had to be different or have a different impact than for all previously known AGNs. For both the rare high-power quasars observable across the whole visible Universe and the more common Seyfert galaxies, well-understood models of accretion disks could be computed (Shakura & Sunyaev 1973; Narayan & Yi 1994). Various explanations for the LINERs were put forward, ranging from shock-ionisation (Heckman 1980) via young hot stars (Terlevich & Melnick 1985) to the favoured ionisation by low-luminosity AGNs (Ferland & Netzer 1983; Halpern & Steiner 1983). The latter explanation has strong implications, because LINERs make up most objects in the AGN class. While in the following decades the explanation that LINERs are powered by low-luminosity AGNs became generally accepted, doubts were again re-fuelled very recently. Inconsistencies were found between the AGN-ionisation hypothesis, and either predicted emission line strengths (Cid Fernandes et al. 2011) or the spatial dis-

tribution of LINER-like ionised regions in the galaxies (Sarzi et al. 2010; Yan & Blanton 2012), but neither were conclusive, because they either lacked full spatial or spectral information.

In this work, we base our analysis on a new dataset that combines a complete spectral and spatial view on LINER galaxies for the first time. We test the picture of ionisation of the gas in these galaxies by an AGN as our null-hypothesis, which geometrically defines illumination by a single central point source. This geometry predicts a radiation field declining in radius as  $\propto 1/r^2$ . With interstellar gas density in galaxies normally distributed in a thin disk with an exponential fall off in radius (Bigiel & Blitz 2012), the density of ionised gas and hence surface brightness of emission line flux should also fall off similar to  $1/r^2$  or faster, if LINER-like emission across the galaxy were caused by a central AGN point-source. If the surface brightness of spatial regions with LINER-like emission falls off less steeply than  $\propto 1/r^2$ , then it is not reconcilable with illumination by an AGN.

For this test, both the full spatial resolution of the galaxies as well as the ability to spectrally identify LINER-like emission by means of diagnostic emission line ratios (Heckman 1980) is required. Whereas either no full spatial component was available (Cid Fernandes et al. 2011; Yan & Blanton 2012) or spectral cov-

\* Member of IMPRS for Astronomy & Cosmic Physics at the University of Heidelberg

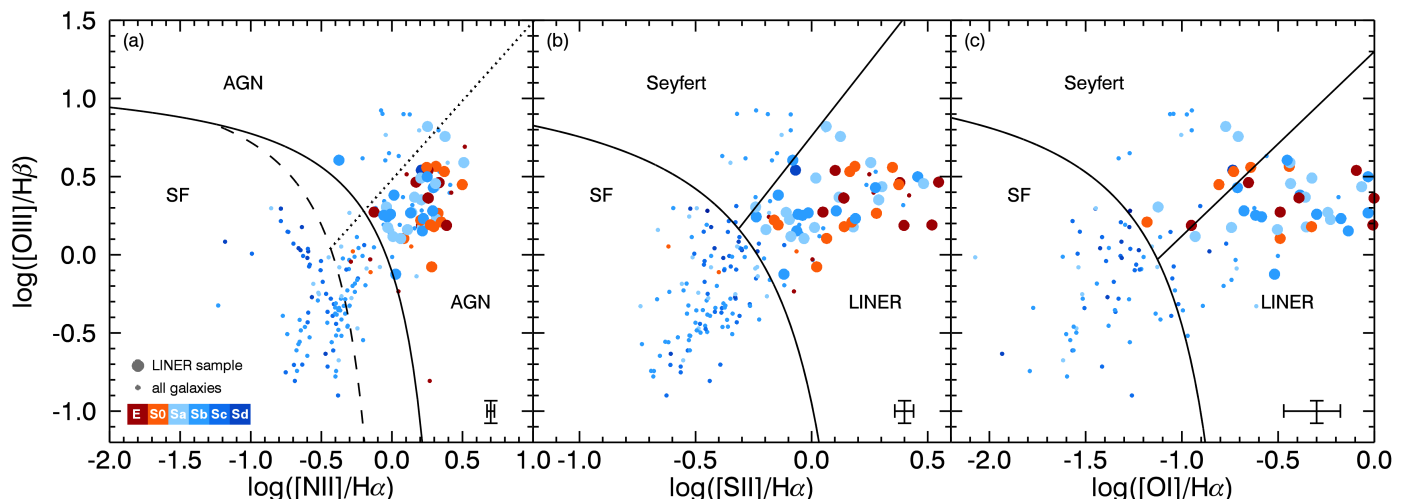


**Fig. 1. Selection of LINER galaxies.** Data points are coloured by Hubble type and show central emission line ratios of 257 CALIFA galaxies on the BPT diagram. Those classified as AGN in (a) and LINER in (b) have larger symbol sizes and are selected for further analysis. Small symbol sizes in the LINER region may appear due to either an inconsistent BPT classification, this typically affects points near the demarcation lines, which are either LINERs in (b) but not AGN in (a), vice versa, or objects that have had the central measurement detect only one of either [NII] or [SII] emission lines. Panel (c) is shown for illustration but not used in the classification due to the larger relative error indicated in the lower right corner of each panel. The solid curves are the theoretically modelled "extreme starburst line" (Kewley et al. 2001). The dashed curve (Kauffmann et al. 2003) and the dotted line (Cid Fernandes et al. 2010) in (a) and the solid lines (Kewley et al. 2006) in (b) and (c) are tracing a minimum in the central emission-line-ratio-distribution of SDSS galaxies.

erage for the LINER diagnostic was limited before (Sarzi et al. 2010), the CALIFA survey (Sánchez et al. 2012; Husemann et al. 2013) provides the first dataset of this kind for a substantial number of LINER galaxies (see also Kehrig et al. 2012).

In Section 2, basic information about the CALIFA survey is provided. In Section 3, we describe our sample selection and the steps of our analysis. In Section 4, we discuss different effects, which might influence our results and show that they are robust against them. We conclude in Section 5 and discuss the implications of our results.

## 2. The CALIFA survey

The Calar Alto Legacy Integral Field Area (CALIFA; Sánchez et al. 2012) survey is the first and ongoing IFS survey of a diameter-selected ( $45'' < D_{25} < 80''$ ) sample of up to 600 galaxies in the local universe ( $0.005 < z < 0.03$ ) of *all Hubble types*. The data are being obtained with the integral-field spectrograph PMAS/PPak mounted on the 3.5 m telescope at the Calar Alto observatory. Its field-of-view of  $65'' \times 72''$  covers the full optical extent of the selected galaxies. More than 96% of the CALIFA galaxies are covered to at least two effective radii. The coverage distribution peaks around  $4 R_e$  and reaches up to  $7 R_e$  for highly inclined galaxies.

This survey comprises two different gratings for each galaxy: one at a lower spectral resolution (V500) of  $6.0 \text{ \AA}$  FWHM and one at a higher resolution (V1200) of  $2.3 \text{ \AA}$  FWHM. Since our specific analysis requires almost the whole optical wavelength range, only the V500 data are used, which cover a nominal wavelength range of  $3745\text{--}7500 \text{ \AA}$  at a median spatial resolution of  $3''.7$ .

The medium-resolution V1200 grating yields high-quality maps of stellar and ionised gas kinematics. The combination with the low-resolution V500 grating allows for mapping of stellar ages, metallicities, full star-formation histories, ionised-gas emission line fluxes, and chemical abundances (e.g. Pérez et al. 2013; Sánchez et al. 2013; Falcón-Barroso et al. in prep.).

The minimal S/N of the spatially-binned V500 spectra used in this analysis was set to 10. Since most spaxels have much higher S/N values, binning was only necessary in the galaxies peripheral areas.

## 3. Spatially resolved LINER-like emission

Among the first 257 galaxies observed within the CALIFA survey, we found 48 LINER galaxies based on their measured central emission line ratios, covering a  $3''$  diameter aperture. These galaxies cover almost all morphological types based on the averages of five independent visual classifications of SDSS  $r$  and  $i$  band images. Based on the ionisation strength and hence the underlying ionisation source, the so-called BPT diagram (Baldwin et al. 1981) is an empirically derived diagnostic tool to distinguish between star formation (dominated by Balmer  $H\alpha$  and  $H\beta$  lines), Seyfert galaxies (with high ionisation potential) and LINER galaxies (with low ionisation lines).

As shown by this diagnostic diagram in Fig. 1, the flux in the lower-ionisation lines  $[\text{NII}]\lambda 6583$ ,  $[\text{SII}]\lambda 6716,31$  and  $[\text{OI}]\lambda 6300$  when compared to  $H\alpha\lambda 6563$  is too high for ionisation by young massive stars, and at the same time, the flux in  $[\text{OIII}]\lambda 5007$  when compared to  $H\beta\lambda 4861$  is too low for ionisation around a typical Seyfert-like medium-luminosity AGN. The emission lines that are combined in the ratios are close in wavelength; therefore, attenuation by dust cancels out, leaving the galaxies to be classified as LINERs.

Subsequently, we measured emission line ratios in different regions across the galaxy for each of these LINER galaxies. Even the weak emission lines can be robustly recovered as we are simultaneously fitting the stellar continuum and emission lines, while requiring a minimum signal-to-noise of 10 per pixel; in the outer parts we combine spectra from neighbouring regions to reach this minimum signal-to-noise. As illustrated for three example galaxies in Fig. 2, we can then place all regions with reliable measured line ratios on the BPT diagrams and classify each of them. Next, we can colour-code all regions across the

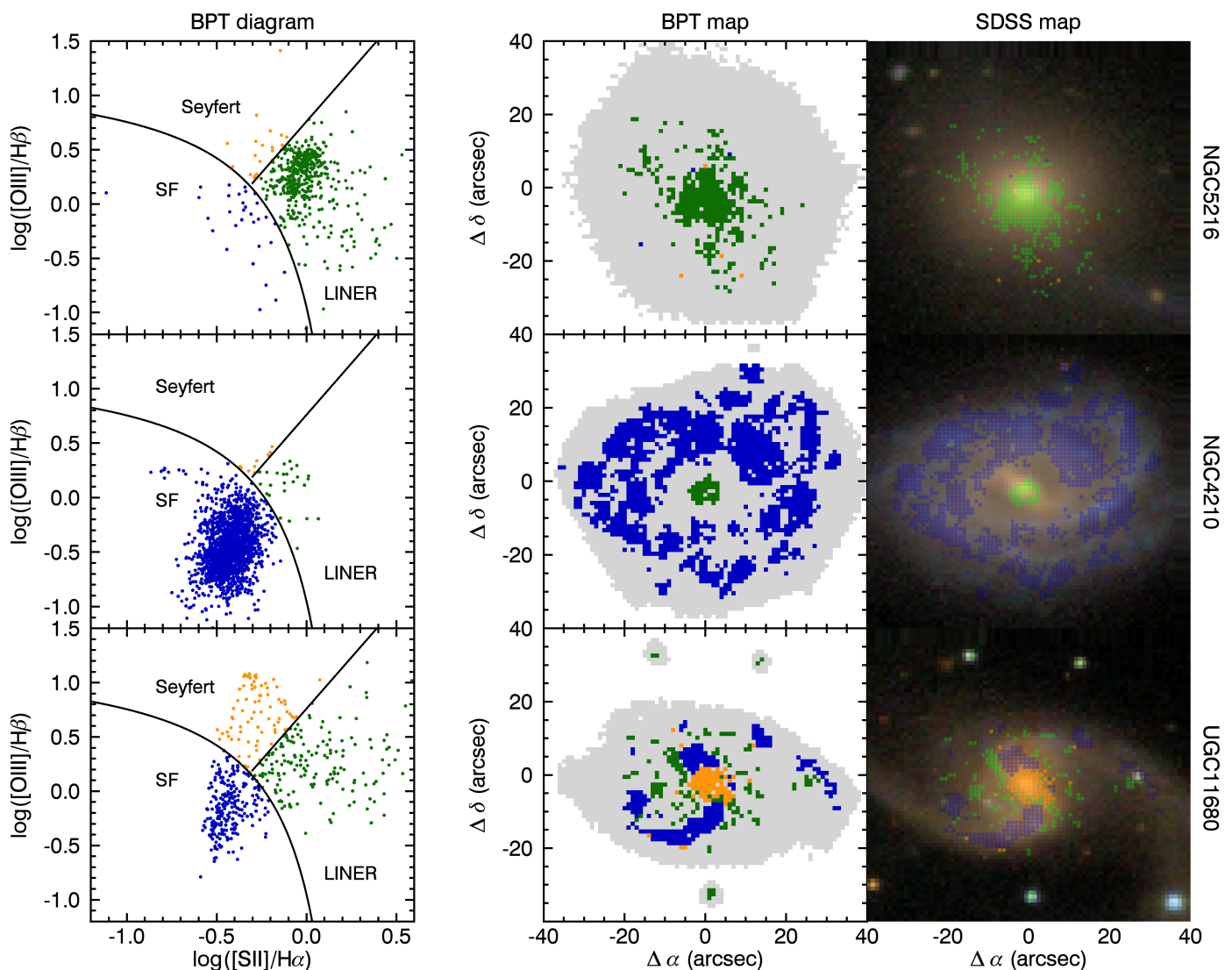


**Fig. 2. Emission-line-ratio classification of spatial regions.** The distribution of measured emission line ratios in a BPT-diagram (left column) and spatially across the galaxy (middle column, usable data regions in grey) differ between example galaxies dominated by LINER-like emission (NGC 5216, top row), a galaxy dominated by star-formation (NGC 4210, middle row) and an AGN in a spiral host (UGC 11680, bottom row). The latter one is shown as an example but not part of our sample. Regions are colour-coded according to their position in the BPT diagram: green for LINER-like, orange for Seyfert-like, and blue for star-formation-like emission line ratios. Overlay of these regions onto the colour-composite image from the SDSS (right column) reveals how LINER-like emission is spatially extended, except when dominated by Seyfert-like emission in the centre or by star-formation-like emission in spiral arms or the disk.

galaxy according to this classification to obtain BPT maps. This map reveals which parts of the galaxy are dominated by star-formation-like emission (typically in the outer parts and/or in spiral arms), Seyfert-like emission (restricted to the centre), or LINER-like emission (typically extended well beyond the nucleus).

Finally, we select only those regions with LINER-like emission and plot the measured  $H\alpha$  surface brightness – or that of any other emission line – versus the distance of each region from the galaxy centre. After normalising the central  $H\alpha$  flux to unity for all galaxies, we arrive at the (smoothed) coloured radial profiles in Fig. 3. The expected profile from central point-source illumination is plotted in black. There is a strong gap between the latter predicted point-source-illumination profile and the actual observed profiles, which increase to  $\geq 1$  dex toward the  $\sim 30''$  radial extent of our data. In some regions, part of the emission can be the result of a superposition of different ionising flux sources.

In Section 4, we describe tests, which assure that the discrepancy between data and the null hypothesis model is not due to this contribution. These tests show that our results are not affected by a potential contribution to the line flux triggered by young stars. The vertical grey lines in Fig. 3 illustrate the radial extent covered by a  $3''$ -diameter SDSS aperture, if the CALIFA galaxies with an average redshift of  $0.017 \pm 0.006$  would be placed at the indicated higher redshifts. This illustrates that SDSS emission line classifications can be non-unique and dependant on redshift, meaning that for example NGC 4210 from Fig. 2 could be classified as either star-forming or LINER galaxy, depending on its distance and hence, apparent size.

In addition, we tested against projection effects for the disk-dominated galaxies in our sample, which affects both radius coordinates and flux densities. After these tests the discrepancy between observed radial line surface brightness profiles and the null hypothesis remains for both early- and late-type galaxies,

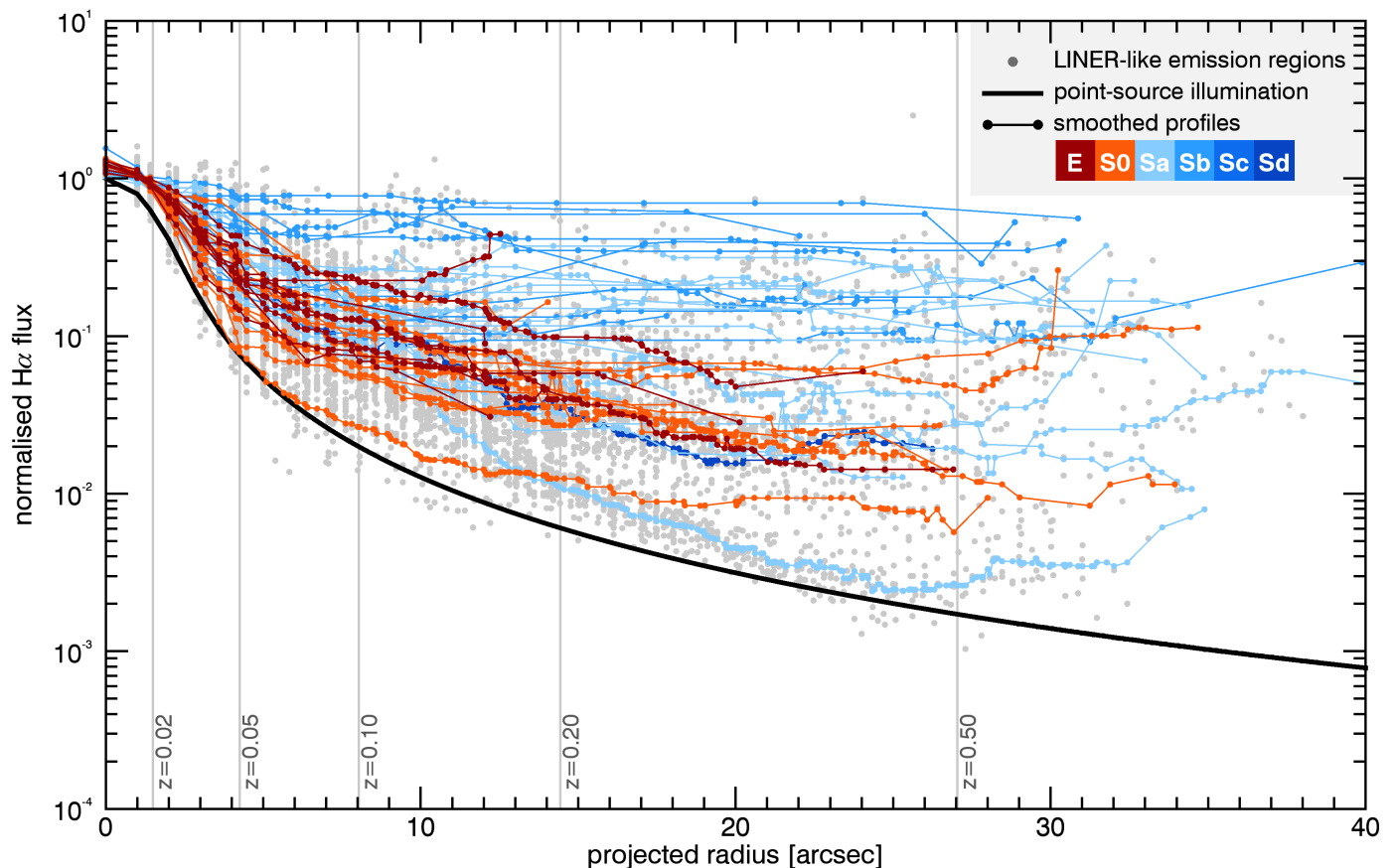


**Fig. 3. Radial profiles of LINER-ionised  $H\alpha$  flux.** The coloured curves are normalised and smoothed radial surface brightness profiles of the  $H\alpha$  emission line flux from our 48 LINER galaxies and compared to a PSF convolved point-source illumination  $1/r^2$ -profile in black. All profiles are normalised with respect to the central flux inside a  $1''.5$  radius aperture. Different colours represent different morphological types ranging from round elliptical galaxies (dark red) to disk-dominated spiral galaxies (dark blue), with lighter colours in-between. Beyond the inner few arcsec for LINER galaxies of all types, there is a significant excess, with up to two orders of magnitude, above the prediction from a point-source ionisation. The vertical grey lines illustrate the radial extent covered by a  $3''$ -diameter SDSS aperture when the CALIFA galaxies with  $\bar{z} = 0.017 \pm 0.006$  would be placed at the indicated higher redshifts.

hence rejecting the model that a central AGN is causing the spatially extended LINER-like emission.

#### 4. Verifying the robustness of our analysis

Below, we discuss various effects that could influence our results and verify that our findings are robust against them.

##### 4.1. Robustness of weak emission line extraction

A central technical part of this work is the extraction of weak emission lines in the presence of a stellar continuum. Since the equivalent width of the lines is often low, specifically with the Balmer  $H\beta$  line being superposed on an absorption trough, an unbiased extraction is the core of the present analysis.

We have employed three different procedures for line extraction. All avoid to model the line flux after a previous subtraction of the stellar continuum. Instead, continuum and line emission are modelled simultaneously, which provides the least-biased line measurement (Sarzi et al. 2006). To assess whether systematics in the line measurement are present and whether the uncertainties on line fluxes – and hence line ratios – are properly derived, we compared the extracted line fluxes and errors from the following complementary approaches:

(a) We use the **gas and absorption-line fitting** procedure GANDALF (Sarzi et al. 2006) with the MILES (Sánchez-Blázquez et al. 2006; Falcón-Barroso et al. 2011) library of stellar templates. In this case, the best fit to a spectrum is the superposition of an optimal combination of the stellar templates with additional Gaussians representing the emission lines. Unfortunately, the GANDALF routine only computes errors for those emission lines that are unrestricted in their kinematical properties. Emission lines that are being tied to another line in either velocity or velocity dispersion are better recovered (Sarzi et al. 2006) but do not come with errors for the measured fluxes.

(b) Same as (a) but we used the MILES library of single stellar populations (SSP) instead of the MILES stellar template library.

(c) To acquire flux errors for all emission lines of interest, we employed a Monte-Carlo simulation, perturbing the input spectrum one hundred times. This amount of different realisations is sufficient to create a Gaussian distribution in extracted fluxes from which we take the mean and standard deviation as measured flux and error value. To make this process computationally feasible, we use the best-fit composite stellar spectrum from a previous emission-line masked stellar continuum fit with the procedure PPXF (Cappellari & Emsellem 2004) instead of the full template library.

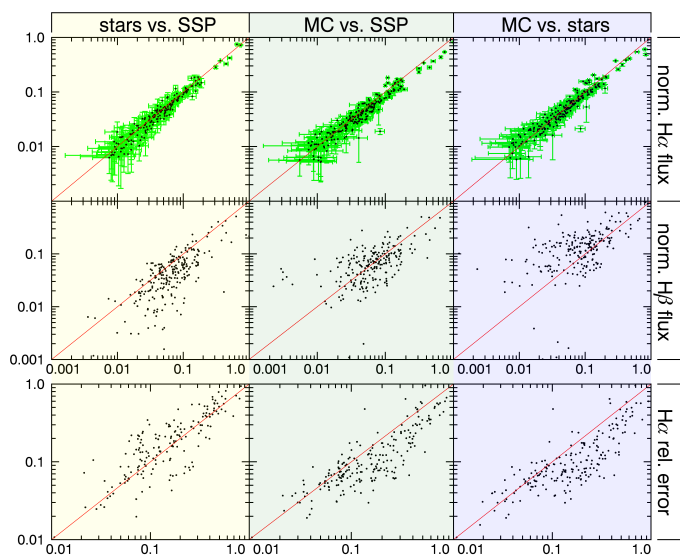


**Fig. 4.** Comparison of extracted  $H\alpha$  fluxes,  $H\beta$  fluxes and estimated errors for the  $H\alpha$  line of NGC 5614, as extracted by Gandalf using the MILES stellar template library, the SSP library and a Monte Carlo variation of noise in the spectra. There is a very good match in the line fluxes between the three methods for the  $H\alpha$  line (row 1), while the errors estimated by Gandalf are larger than the statistical variance from the Monte Carlo approach (row 3). The weak  $H\beta$  line is generally better recovered using either the Monte-Carlo or GANDALF/SSP method (row 2).

As an example in Fig. 4, the resulting fluxes and errors are compared for the  $H\alpha$  and  $H\beta$  line of NGC 5614. There is no systematic difference in flux extraction between the three methods also at the faint end with a scatter within each method’s uncertainty. The  $\chi^2$ -based error from GANDALF, most likely due to unaccounted small pixel-to-pixel systematics and correlations, are larger than the robust Monte Carlo measurements. We verified that even if the Monte Carlo errors happened to be underestimated our results are unchanged, and we conclude that the line flux properties are accurately measured, down to the faintest end.

#### 4.2. Point source radiation to radial flux profile

The radiation field from a central point source like an AGN declines with the inverse of the radial distance  $\propto 1/r^2$ . In the case that the photo-ionised gas is optically thin and distributed in an infinitesimally thin disk with a constant filling factor and constant density, the resulting observed emission-line flux also falls off inversely squared with (projected) radius  $\propto 1/R^2$ .

The fall-off is even faster when the gas is not optically thin and part of the ionisation gets absorbed by intervening gas (clouds). Similarly, a radially decreasing filling factor results in a faster decline, whereas the opposite of an increase would require very special conditions. With perhaps the exception of strongly interacting galaxies, the gas density in galaxies is normally radially decreasing (Bigiel & Blitz 2012), so that the flux is also expected to drop at an even faster gradient than inverse square in this case. Only in the case that the thin-disk assumption is strongly invalidated do we expect the opposite effect of a decline shallower than  $\propto 1/R^2$  – in the extreme case of optically thin gas with a constant filling factor and constant density in a spherical distribution, the line-of-sight integral results in an observed

emission-line flux that will fall off inversely linear with projected radius.

However, the resulting kinematics in all types of galaxies with (ionised) gas present shows clear disk-like rotation, apart from disturbances due to non-axisymmetric structures (bars and spiral arms) and tidal interactions (e.g., Garcia-Lorenzo et al., in prep.). The resulting angular momentum implies that the gas always settles in a disk, which, however, can have a substantial thickness. After line-of-sight integration, the latter thickness still results in a slightly slower fall-off than the inverse square, but the radially declining gas density typically compensates for this.

We illustrate the latter by a simple model in which a central point source ionises optically thin gas with a constant filling factor distributed in an axisymmetric disk viewed at an inclination angle  $i = 60^\circ$  (with  $i = 0^\circ$  face-on and  $i = 90^\circ$  edge-on). Combined neutral and molecular hydrogen measurements in nearby galaxies show that the gas density declines exponentially in radius (Bigiel & Blitz 2012) and that the vertical fall-off is typically well matched by an exponential as well. Henceforth, we adopt a double-exponential for the gas density  $\propto \exp[-R/h_R] \exp[-|z|/(q h_R)]$  with fiducial values for the scale length of  $h_R = 3$  kpc and for the flattening of  $q = 0.1$ . The resulting flux profile is shown in Fig. 5 as the thick dashed curve, whereas the thin long/short dashed curves show the effect of a factor two thicker/thinner disk. The differences with respect to the  $1/R^2$  fall-off (thick solid curve) are much smaller than the offset from the on average, much shallower observed flux profiles shown in Fig. 3. The same holds true for a thin disk ( $q = 0.1$ ) with a much larger scale length ( $h_R = 5$  kpc), as indicated by the dash-dotted curve, or a spherical ( $q = 1$ ) and more centrally concentrated ( $h_R = 1$  kpc) gas distribution, represented by the dotted curve.

#### 4.3. Impact of geometric projections

Even if the disks of galaxies are intrinsically round, the inclination at which we observe them results in projection effects that act both on the minor axis radius coordinate and the effective gas density and hence, line emitting region. Under the assumption of a geometrically thin gas distribution, a proper de-projected radius would be described by  $\sqrt{R_a^2 + (R_b/\cos i)^2}$  with a major-axis radius component  $R_a$ , observed minor axis component  $R_b$ , and inclination angle  $i$ . The gas distribution itself, on the other hand, would be projected by the same amount as the minor axis component,  $\cos i$ . Hence, the observed projected profiles have all data points moved to smaller observed radii by different amounts, while the flux density is moved to higher values.

To assess whether this produces a significant net increase or decrease of the difference between observations and models as seen in Fig. 3, a tentative and maximal de-projection of all disk-dominated galaxies in our sample was carried out for illustrative purposes, as shown in Fig. 6. For this calculation, we adopted  $\cos i = 1 - \epsilon$  for a thin disk with observed ellipticity  $\epsilon$  that is derived from an isophotal analysis of the SDSS images. As can be seen, the impact on the discrepancy model–observations is at most small, and it can be concluded that projection effects play no significant role in the interpretation.

#### 4.4. Impact of mixed-in star formation contribution

A selection of spaxels in a BPT diagram above the theoretical upper limit of where star formation alone can produce given line ratios does not preclude a significant contribution to the line

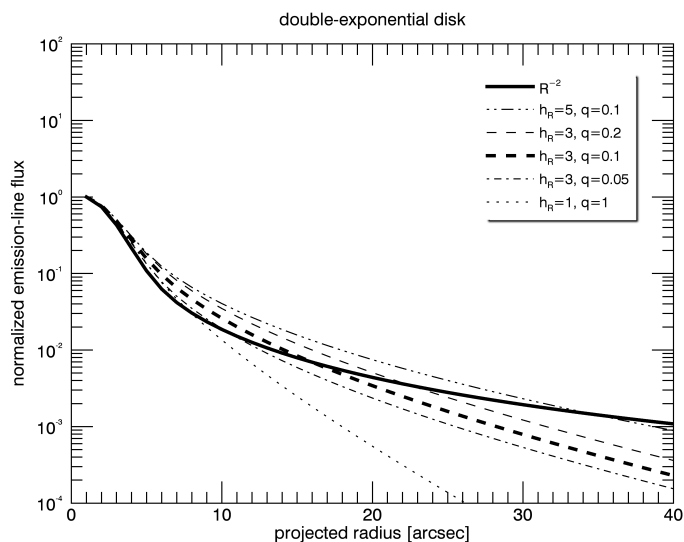


**Fig. 5.** Normalised flux profiles as a function of projected radius  $R$  of gas being ionised by a central point source. The thick solid curve assumes that the gas is optically thin and distributed in an infinitesimally thin disk with a constant filling factor and constant density, so that the fall-off is the same inversely squared with radius as the point-source radiation. The thick dashed curve is when the gas is distributed in an axisymmetric disk of finite thickness with gas density both radially and vertically declining exponentially as  $\propto \exp[-R/h_R] \exp[-|z|/(q h_R)]$  with fiducial values for the scale length of  $h_R = 3$  kpc and for the flattening of  $q = 0.1$ , viewed at an inclination angle of  $i = 60^\circ$ . The thin long/short dashed curves show the effect of a factor of two thicker/thinner disk, the dash-dotted curve is for when the scale length is much larger, and the dotted curve is when the gas distribution is spherical and more centrally concentrated.

emission from star formation (SF). In principle, a mix of a fiducial “pure LINER” with a “pure SF” ionising radiation field, can lead to substantial SF contribution to the emission line flux outside the classical SF region. Given that early-type galaxies with negligible SF show similarly shallow flux profiles as late-type galaxies with significant SF (Fig. 3), this result already hints that mixed-in SF contributions cannot be the source of the discrepancy with a point-source illumination.

Even so, we estimate the level of mixed-in SF contribution by assuming that the observed emission-line fluxes are a linear combination of flux  $F_L$  from “pure LINER” ionisation and flux  $F_{SF}$  from “pure SF” ionisation. The line ratios from these pure ionisation sources correspond to points in the LINER and SF regimes of the BPT diagrams. For a given  $H\beta$ -to- $H\alpha$  flux ratio, the so-called Balmer decrement, which increases the ratio  $F_{SF}/F_L$  from zero, traces a curve from the pure LINER point toward the pure SF point in the BPT diagram, as illustrated in Fig. 7.

As the latter pure SF points (blue stars), we use locations on the SF-ridge of SDSS galaxies (Kewley et al. 2006) that are shown as grey levels in the background. We infer to the pure LINER point (orange point), from the average position of the nine elliptical LINER galaxies from our sample. These elliptical galaxies are devoid of any SF, but there could still be mixed-in ionisation contribution from a central AGN in their inner regions. Indeed, computing the position based on emission-line fluxes from different galactocentric annuli shows that the two central-most annuli (dark-red and red points) yield a position more toward the Seyfert regime. The average position resulting from the

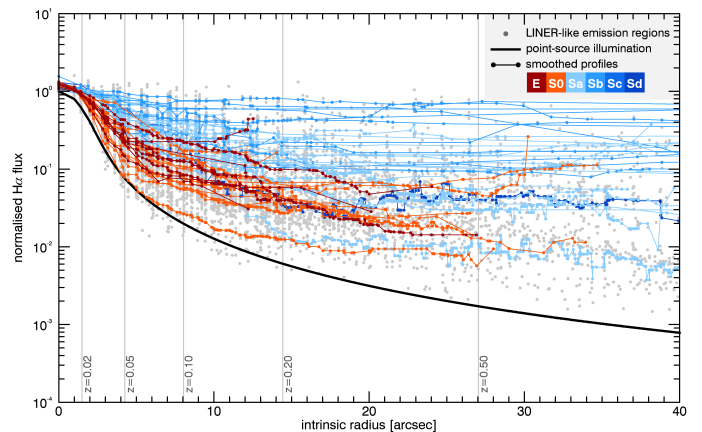


**Fig. 6.** De-projection of radial  $H\alpha$  surface brightness profiles. To demonstrate how strongly potential projection effects of galaxy inclination could impact our results, all disk-dominated galaxies of the sample were subjected to a maximal geometrical de-projection. For this test, it was assumed that these galaxies were infinitely thin disks and that observed ellipticities were fully due to an inclination of the disk with respect to the observer’s line of sight. Both radius and gas surface density projection were considered. The comparison to Fig. 3 shows a stretch of the radius axis for some objects, but neither qualitative nor quantitative difference in surface brightness excess for the galaxies over the point-source line is shown.

annuli further out nicely converge to the same position, again in-line with ionisation by the same but non-central sources.

To go from this pure LINER point to the black solid demarcation line, the SF-to-LINER flux ratio increases to  $F_{SF}/F_L = 0.2$ , so that a maximum of 1/6th of observed flux could be due to mixed-in SF contribution. The resulting decrease in the observed flux is negligible with respect to the offset from the point-source illumination in Fig. 3. Placing the pure LINER point further away from the demarcation line increases the possible SF-to-LINER flux ratio. Given the spread in the convergence point among the elliptical galaxies (orange cross), however, we find  $F_{SF}/F_L < 0.5$ . Hence only 1/3rd of the observed flux could still be due to mixed-in SF contribution, and we conclude that, SF cannot be a significant source of the observed shallow emission-line flux profiles even for the spiral galaxies, whereas ionisation from the same common old stars forms the natural explanation.

## 5. Discussion and Conclusions

For 48 galaxies with LINER-like emission we unambiguously show, that the class of LINER galaxies, contrary to their 30-year old paradigm, are not predominantly powered by a central AGN, since their radial emission-line surface brightness profiles are inconsistent with ionisation by a central point-source and hence cannot be due to an AGN alone. When using this result in reverse, we conclude that the power source for LINER-like emission must be extended, which is possibly distributed all through the galaxy, while it is clear that an adequate supply of gas is indispensable for such line emission to exist in the first place. Despite its name LINER-like emission covers all regions of the galaxies, aside from those where star-formation dominates the emission. There is also no spatial collimation as would be expected in the case of shock-driven ionisation. Henceforth, the most probable energy source are hot evolved stars after their asymptotic giant branch (AGB) phase. This was already suggested before (Binette et al. 1994; Goudfrooij 1997, 1999), but models of this phase in stellar evolution have only recently been

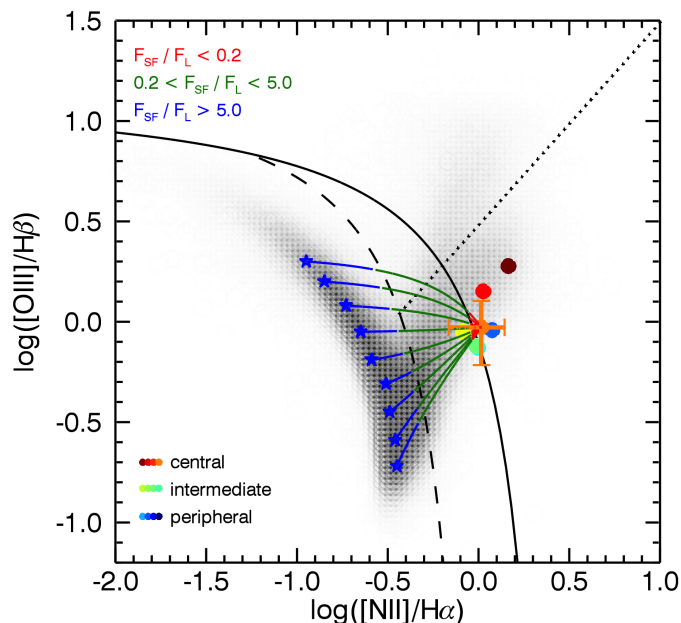


**Fig. 7.** Resulting line ratios if line emission flux purely from SF (blue stars) and purely from a LINER mechanism (orange point) are linearly superposed (coloured lines). The generating  $H\alpha$  flux ratios are colour coded. This shows that the SF contribution in the selected LINER regime right of the solid curve is negligible ( $F_{SF}/F_L < 0.2$ ) and cannot be generating the discrepancy seen in radial emission line profiles with respect to a point-source illumination of  $>1$  dex at larger radii.

picked up again (Stasińska et al. 2008). After stars leave their main sequence of hydrogen burning, and after a few subsequent evolutionary stages, they enter the so-called AGB. In the following post-AGB phase, the stars can become sufficiently hot to produce a spectrum capable of ionising atoms with a substantial ionisation potential. Realising this has the perplexing implication that every galaxy for both early- and late-type galaxies with stellar populations older than  $\sim 1$  Gyr must have a radiation field from post-AGB stars that can ionise at least part of the interstellar gas when present.

Even if central or extended LINER-like emission is predominantly powered by post-AGB stars, it does not preclude the existence of AGNs in LINER galaxies. The AGN could provide some of the central radiation in some LINER galaxies, which may even host a higher fraction of AGN compared to the general population of massive galaxies (González-Martín et al. 2009): The reason for this could in the simplest case be a selection effect due to the required presence of central reservoirs of gas and hence potential for it being accreted onto a central black hole. However, many galaxies with LINER-like emission do not have a central AGN. This shows that the LINER diagnostic is in general not a good predictor for the presence of an AGN.

In addition, relying on LINER signatures for AGN selection suffers from aperture effects: Observing galaxies at different distances therefore different physical apertures (see Fig. 3) clearly makes a comparison of the properties even of classical LINERs difficult because of the mixing of signals from emitting regions at different radii.

This emphasises that LINERs or galaxies with widespread LINER-like emission are not just a mixed bag of properties but are mainly just normal galaxies with some gas content in the absence of substantial ionisation fields from young stars and AGN.

The consequences are profound for different fields in astrophysics, ranging from galaxy evolution models, which have hot old stars as an always-present ionisation source that create LINER-like emission whenever gas is present, to black hole studies, which do not have to resort to rare accretion models to explain the LINER galaxies. The three immediate consequences from this result are described below.

First, the ubiquitous presence of ionising radiation from post-AGB stars means that *galaxies with LINER-like emission are not a class defined by a property, but rather by the absence of a property*, or the absence of a stronger radiation field, as for example produced by young stars. This both explains why typical LINER galaxies are massive and old: These are the only galaxies without substantial star formation and with enough post-AGB stars to generally detect the LINER signature (Papaderos et al. 2013). This also tells us why LINERs appeared as a mixed bag: The presence of other sources of energy – AGN, star formation, shocks – is actually completely independent of the source powering the LINER signature.

Second, we need to revisit the properties of classical AGN host galaxies, since a number of studies in the past decade used, for example, the SDSS survey to investigate AGN host galaxies in the local Universe. Since the sample selection LINERs outnumber classical Seyferts 5:1, were often counted into the AGN class (Kauffmann et al. 2003; Kauffmann & Heckman 2009; Schawinski et al. 2007), and were being impacted by the different physical apertures covered at different redshifts (Fig. 3), these studies might have come to biased results.

Third, with LINER-signatures now being removed as a self-contained AGN indicator, the family of AGN becomes much smaller and simpler.

*Acknowledgements.* The authors would like to thank all of the CALIFA collaboration for their input, Brent Groves for very useful discussions on ionisation properties and Remco van den Bosch for his technical and scientific advises. RS acknowledges support by the IMPRS for Astronomy & Cosmic Physics at the University of Heidelberg. KJ is supported by the Emmy Noether-Programme of the German Science Foundation DFG under grant Ja 1114/3-2 and the German Space Agency DLR. G. v. d. V. and J. F.-B. acknowledge the DAGAL network from the People Programme (Marie Curie Actions) of the European Union's Seventh Framework Programme FP7/2007-2013/ under REA grant agreement number PITN-GA-2011-289313. J. F.-B. further acknowledges financial support from the Ramón y Cajal Program and grant AYA2010-21322-C03-02 from the Spanish Ministry of Economy and Competitiveness (MINECO). VW acknowledges support from the ERC Starting Grant SEDmorph. R. A. Marino was also funded by the Spanish programme of International Campus of Excellence Moncloa (CEI). This study makes use of the data provided by the Calar Alto Legacy Integral Field Area (CALIFA) survey (<http://califa.caha.es/>) and is based on observations collected at the Centro Astronómico Hispano Alemán (CAHA) at Calar Alto, operated jointly by the Max-Planck-Institut für Astronomie and the Instituto de Astrofísica de Andalucía (CSIC).

## References

- Baldwin, J. A., Phillips, M. M., & Terlevich, R. 1981, *PASP*, 93, 5
- Bigiel, F. & Blitz, L. 2012, *ApJ*, 756, 183
- Binette, L., Magris, C. G., Stasińska, G., & Bruzual, A. G. 1994, *A&A*, 292, 13
- Cappellari, M. & Emsellem, E. 2004, *PASP*, 116, 138
- Cid Fernandes, R., Stasińska, G., Mateus, A., & Vale Asari, N. 2011, *MNRAS*, 413, 1687
- Cid Fernandes, R., Stasińska, G., Schlickmann, M. S., et al. 2010, *MNRAS*, 403, 1036
- Falcón-Barroso, J., Lyubenova, M., & van de Ven, G. in prep., *A&A*
- Falcón-Barroso, J., Sánchez-Blázquez, P., Vazdekis, A., et al. 2011, *A&A*, 532, A95
- Ferland, G. J. & Netzer, H. 1983, *ApJ*, 264, 105
- González-Martín, O., Masegosa, J., Márquez, I., Guainazzi, M., & Jiménez-Bailón, E. 2009, *A&A*, 506, 1107
- Goudfrooij, P. 1997, in *Astronomical Society of the Pacific Conference Series*, Vol. 116, *The Nature of Elliptical Galaxies; 2nd Stromlo Symposium*, ed. M. Arnaboldi, G. S. Da Costa, & P. Saha, 338

- Goudfrooij, P. 1999, in *Astronomical Society of the Pacific Conference Series*, Vol. 163, *Star Formation in Early Type Galaxies*, ed. P. Carral & J. Cepa, 55
- Halpern, J. P. & Steiner, J. E. 1983, *ApJ*, 269, L37
- Heckman, T. M. 1980, *A&A*, 87, 152
- Husemann, B., Jahnke, K., Sánchez, S. F., et al. 2013, *A&A*, 549, A87
- Kauffmann, G. & Heckman, T. M. 2009, *MNRAS*, 397, 135
- Kauffmann, G., Heckman, T. M., Tremonti, C., et al. 2003, *MNRAS*, 346, 1055
- Kehrig, C., Monreal-Ibero, A., Papaderos, P., et al. 2012, *A&A*, 540, A11
- Kewley, L. J., Dopita, M. A., Sutherland, R. S., Heisler, C. A., & Trevena, J. 2001, *ApJ*, 556, 121
- Kewley, L. J., Groves, B., Kauffmann, G., & Heckman, T. 2006, *MNRAS*, 372, 961
- Narayan, R. & Yi, I. 1994, *ApJ*, 428, L13
- Papaderos, P., Gomes, J., Vílchez, J., et al. 2013, *A&A*
- Pérez, E., Cid Fernandes, R., González Delgado, R. M., et al. 2013, *ApJ*, 764, L1
- Sánchez, S. F., Kennicutt, R. C., Gil de Paz, A., et al. 2012, *A&A*, 538, A8
- Sánchez, S. F., Rosales-Ortega, F. F., Jungwiert, B., et al. 2013, *A&A*, 554, A58
- Sánchez-Blázquez, P., Peletier, R. F., Jiménez-Vicente, J., et al. 2006, *MNRAS*, 371, 703
- Sarzi, M., Falcón-Barroso, J., Davies, R. L., et al. 2006, *MNRAS*, 366, 1151
- Sarzi, M., Shields, J. C., Schawinski, K., et al. 2010, *MNRAS*, 402, 2187
- Schawinski, K., Thomas, D., Sarzi, M., et al. 2007, *MNRAS*, 382, 1415
- Shakura, N. I. & Sunyaev, R. A. 1973, *A&A*, 24, 337
- Stasińska, G., Vale Asari, N., Cid Fernandes, R., et al. 2008, *MNRAS*, 391, L29
- Terlevich, R. & Melnick, J. 1985, *MNRAS*, 213, 841
- Yan, R. & Blanton, M. R. 2012, *ApJ*, 747, 61

- 
- <sup>1</sup> Max-Planck-Institut für Astronomie (MPIA), Königstuhl 17, 69117 Heidelberg, Germany
- <sup>2</sup> Instituto de Astrofísica de Canarias (IAC), E-38205 La Laguna, Tenerife, Spain
- <sup>3</sup> Depto. Astrofísica, Universidad de La Laguna (ULL), 38206 La Laguna, Tenerife, Spain
- <sup>4</sup> University of Vienna, Türkenschanzstrasse 17, 1180 Vienna
- <sup>5</sup> Departamento de Física, Universidade Federal de Santa Catarina, PO Box 476, 88040-900 Florianópolis, SC, Brazil
- <sup>6</sup> CENTRA - Centro Multidisciplinar de Astrofísica, Instituto Superior Técnico, Av. Rovisco Pais 1, 1049-001 Lisbon, Portugal
- <sup>7</sup> Instituto de Astrofísica de Andalucía (CSIC), Glorieta de la Astronomía s/n, E18008 Granada, Spain
- <sup>8</sup> Leibniz-Institut für Astrophysik Potsdam (AIP), An der Sternwarte 16, D-14482 Potsdam, Germany
- <sup>9</sup> Centro Astronómico Hispano Alemán, Calar Alto, (CSIC-MPG), C/Jesús Durbán Remón 2-2, E-04004 Almería, Spain
- <sup>10</sup> Astronomisches Rechen Institut, Zentrum für Astronomie der Universität Heidelberg, Mönchhofstrasse 12-14, D-69120 Heidelberg, Germany
- <sup>11</sup> School of Physics and Astronomy, University of St Andrews, North Haugh, St Andrews, KY16 9SS, U.K. (SUPA)
- <sup>12</sup> Institute of Astronomy, University of Cambridge, Madingley Road, Cambridge CB3 0HA UK
- <sup>13</sup> CEI Campus Moncloa, UCM-UPM, Departamento de Astrofísica y CC. de la Atmósfera, Facultad de CC. Físicas, Universidad Complutense de Madrid, Avda. Complutense s/n, 28040 Madrid, Spain